Mean-Field Study of Poly(methacrylic acid) Shells in Partly Hydrophobically Modified Amphiphilic Block Copolymer Micelles in Polar Solvents†

Karel Jelínek, Filip Uhlík, Zuzana Limpouchová, and Karel Procházka*

Department of Physical and Macromolecular Chemistry and Laboratory of Specialty Polymers, School of Science, Charles University in Prague, Albertov 6, 128 43 Prague 2, Czech Republic

Received: November 14, 2002; In Final Form: May 22, 2003

The structure of poly(methacrylic acid) (PMA) shells in polystyrene-*block*-poly(methacrylic acid) (PS−PMA), micelles was studied by self-consistent field (SCF) calculations. The PS−PMA micelles can be modified by naphthalene tags immobilized at the core/shell interface and by hydrophobic anthracene tags at the ends of PMA chains. The nonmodified, partly modified, and 100% hydrophobically modified PS−PMA micelles were studied. Special attention was devoted to the distribution of anthracene tags attached at the ends of PMA blocks in aqueous mixtures with 1,4-dioxane (i.e., in nonpolyelectrolyte regime). The study shows that hydrophobic tags try to avoid the polar solvent and force the PMA chains to loop toward the core. We found that in partly modified micelles, the tags return closer to the core than in 100% tagged micelles because the entropy loss due to the looping is compensated by the conformational behavior of nonmodified PMA chains. The nonradiative energy transfer from naphthalene donors to anthracene traps was treated on the basis of distribution functions obtained by SCF method. The donor fluorescence decays were compared with experimental data published in the accompanying paper. The agreement was found to be good at the semiquantitative level.

Introduction

Water-soluble polymeric micelles and related polymeric nanoparticles have been a subject of numerous studies in the past decade[1−9] because they offer interesting potential applications in various fields, for example, in drug and gene delivery.[10−17] The nanostructures, which were recently designed for gene delivery purposes, are usually complex. Some authors have been considering the attachment of recognition or modifier groups at the ends of water-soluble blocks of amphiphilic block copolymers and the formation of self-assembled micelle-like nanoparticles with incorporated DNA in aqueous media.[18−20] If the recognition groups have amphiphilic character or some degree of hydrophobicity, they do not have to be localized at the periphery of micelles, but their distribution in the shell may be fairly broad and shifted toward the core/shell interface. Therefore, the spatial distribution of modified ends of the shell-forming blocks has to be studied. Because of the complexity of biocompatible nanoparticles, experimental studies on simple, stable, and well-defined model systems and theoretical (Monte Carlo and mean-field) calculations are needed.

Micellization of amphiphilic block copolymers (mostly block polyelectrolytes) has been studied both experimentally[3,21−29] (for more references, see the accompanying paper[30]) and theoretically[31−41] for more than 10 years. Recently, we investigated micellar systems with modified ends of the water-soluble blocks. We studied the 100% tagged micelles formed by polystyrene-*block*-poly(methacrylic acid), PS−N−PMA−A, double tagged by naphthalene between blocks and by anthracene at the end of the PMA block.[42−44] The double tagging is a suitable modification for fluorometric nonradiative energy transfer (NRET) studies and allows for an estimate of the spatial distribution of hydrophobic anthracene tags in the shell. Because the number of recognition groups in realistic micelle-based gene delivery systems is lower than the number of the shell-forming blocks, later we studied also hybrid micelles with only partly modified shells, formed by mixtures of nonmodified PS−PMA and modified PS−N−PMA−A and also by polystyrene-*block*-poly(ethylene oxide) (PS−PEO) and PS−N−PMA−A.[30] In all studied systems, we have found that the hydrophobic pendant anthracene tags return back and bury in the relatively hydrophobic inner shell formed by the nondissociated PMA, forcing the tagged chains to loop back toward the core. The behavior of PS−PMA micelles is further complicated in respect to other types of micelles because PMA is not a typical polyelectrolyte and has some properties of polysoaps.[45−50]

In this paper, we study the distribution of hydrophobic tags in the shell and the distribution of segments of tagged and nontagged chains by mean-field calculations based on the model of Scheutjens and Fleer.[51,52]

Method

Self-Consistent Field Theory. A self-consistent field (SCF) method developed by Scheutjens and Fleer[51,52] was used for studying the modified and nonmodified PMA shells in strongly polar solvents (typically a 1,4-dioxane (30 vol %) mixture with water). The choice of a mixed solvent with a considerable amount of 1,4-dioxane simplifies the study. In such a solvent, the dissociation of COOH groups in PMA is negligible and does not have to be taken into account. The study on micelles in purely aqueous media is in progress and results will be published later.

In the method used, the polymer chains are modeled as the first-order Markov chain, that is, it is assumed that the position of a given segment, *k*, depends only on the position of the

† Part of the special issue "International Symposium on Polyelectrolytes".
* To whom correspondence should be addressed.

10.1021/jp0224463 CCC: $25.00
Published on Web 06/24/2003

immediately preceding segment $k-1$. The steps in all possible directions, including an immediate reversal step, are allowed.

For each unit of type i in the system (i.e., segment of a certain type, hydrophobic pendant group, solvent), we define the weighting factor

$$G_i(z) = \exp[-u_i(z)/(kT)] \quad (1)$$

which is the Boltzmann factor reflecting potential energy, $u_i(z)$, of this segment (or solvent) in layer z. In general, $u_i(z)$ contains a hard-core potential, $u'(z)$, independent of the segment type and an interaction part $u_i^{\text{int}}(z)$, which depends on local concentrations and interaction parameters. Hence, we may write

$$u_i(z) = u'(z) + u_i^{\text{int}}(z) \quad (2)$$

For a chain that contains s segments of the ith type, the end-segment weighting factor, $G_i(z,s)$, can be calculated from $G_i(z)$ through the recurrence formula

$$G_i(z,s+1) = G_i(z)\{\lambda_{-1}G_i(z-1,s) + \lambda_0 G_i(z,s) + \lambda_1 G_i(z+1,s)\} \quad (3)$$

where $G_i(z,1) = G_i(z)$. The parameters λ_1, λ_{-1}, and $\lambda_0 = 1 - \lambda_{-1} - \lambda_1$ are the probabilities that the segment under consideration will cross into the next or into the preceding layer or will remain in the same layer. For a simple cubic lattice, $\lambda_{-1} = \lambda_1 = {}^1/_4$ and $\lambda_0 = 4\lambda_1 = {}^4/_6$. For a spherical lattice, the parameters $\lambda_1(z)$ and $\lambda_{-1}(z)$ depend on the lattice layer and are proportional to the contact area between layers z and $z+1$ and z and $z-1$, respectively. The $\lambda_0(z)$ is calculated from the relation $\lambda_0 = 1 - \lambda_{-1} - \lambda_1$. The segment density, $\Phi_i(z,s)$, of segments s of the ith type component in the layer z may be calculated from $G_i(z,s)$:

$$\Phi_i(z,s) = (C_i/G_i(z))G_i(z,s)G_i(z,r_i-s+1) \quad (4)$$

The normalization constant C_i for the ith component in the equilibrium with the bulk solution is given by $C_i = \Phi_i^{\text{bulk}}/r_i$, where Φ_i^{bulk} is the bulk concentration of the ith component and r_i is the number of segments per one chain. For segments of a grafted polymer, the bulk concentration is zero, that is, $\Phi_i^{\text{bulk}} = 0$, and C_i can be calculated from the following equation: $C_i = \Theta_i/(r_i\sum_z G_i(z,r_i))$, where Θ_i is the total number of segments of ith type. The density of segments i in layer z is calculated as a sum over all segments of type i in layer z (i.e., $\sum_s$ means a summation over a subensemble of segments of the type i in the layer z)

$$\sum_i \Phi_i(z) = 1, \quad \text{where} \quad \Phi_i(z,s) = \sum_s \Phi_i(z,s) \quad (5)$$

Equation 5 reflects the requirement of the full occupancy of all lattice sites in all layers (either by chain segments or solvent). Equations 1−5 form a self-consistent set of equations that can be resolved numerically. In the first step, reasonable initial estimates of $u_i(z)$ for all components in all layers have to be made. It the second step, the distributions $G_i(z)$, $G_i(z,s)$, and finally the segment densities $\Phi_i(z)$ are calculated. The obtained segment density is then used for the calculation of the interaction energy of component i in layer z

$$\langle\Phi_j(z)\rangle = \lambda_{-1}\Phi_j(z-1) + \lambda_0\Phi_j(z) + \lambda_1\Phi_j(z+1) \quad (6)$$

$$u_i^{\text{int}}(z) = \sum_j \chi_{ij}[\langle\Phi_j(z)\rangle - \Phi_j^{\text{bulk}}] \quad (7)$$

If the obtained values meet the boundary condition (i.e., the normalization condition, eq 5) and give the same $u'(z) = u_i(z) - u_i^{\text{int}}(z)$ for each component i, the estimates describe the equilibrium conditions. If not, the iteration procedure is repeated until the equilibrium boundary condition is met.

Model Description and Parameterization. In this paper, we study general trends of the behavior of hydrophobically modified micelles in polar media. We want to reproduce the most important features of the system behavior by our simulations on the semiquantitative level. Nevertheless, we try to get the quantitative agreement between the simulated and experimental data as good as possible. Therefore, we pay special attention to the parametrization of model calculations.

The model mimics the core/shell structure of polymeric micelles with kinetically frozen cores in aqueous media. We model micelles formed by PS−PMA polymers that are similar to those we studied experimentally,[30] that is, the real length of blocks is ca. 600 monomeric units. The association number is set according to experimental scaling law for PS−PMA micelles in a mixed solvent 1,4-dioxane (80%)−water, in which micelles are formed (before they are transferred in the kinetically frozen state in purely aqueous media). In this mild selective mixture, the micelles are formed spontaneously upon dissolution; the sample and micelles with swollen cores coexist in a reversible equilibrium with a low fraction of unimers. Qin and Munk and co-workers studied the micellization of different PS−PMA samples in a mixture of 1,4-dioxane (80%)−water and published the following scaling law[53]

$$N_{\text{ag}} = 0.40 n_{\text{PS}}^{1.89} n_{\text{PMA}}^{-0.86} \quad (8)$$

where n_{PS} and n_{PMA} are numbers of monomeric units of PS and PMA blocks, respectively.

The core of reversible micelles is formed by a swollen PS of the density $0.75\rho_{\text{PS}}$, where 0.75 reflects the experimentally estimated swelling[53] in the mixed solvent under consideration. In water, we assume that the polystyrene core is glassy and has the bulk PS density $\rho_{\text{PS}} = 1.05\ \text{g}\cdot\text{cm}^{-3}$. The core radius R_c is calculated using the estimated association number, the length of the insoluble PS block, and density of either swollen or glassy PS. The shell is formed by PMA chains, which are tethered to the core surface. In the reference system, the shell is a regular convex polyelectrolyte PMA brush. In the hydrophobically modified system, the shell consists of a mixture of regular and modified PMA chains that have hydrophobic anthracene groups attached to their free ends. The modified copolymer contains also one pendant naphthalene group, which is immobilized at the core/shell interface. Because thermodynamic properties of the bridge (2-naphthyl)-1,2-ethylene units are fairly similar to those of PS repeating units, their presence is not important for calculating the structural characteristics, but it plays an important role in NRET calculations. According to experimental findings, we assume that the core/shell interface is very narrow because of the strong incompatibility of PS and PMA blocks. The core/shell interface represents the first spherical layer with $z = 0$ and radius R_c. All chains in the shell are grafted to the core, that is, their ends are placed in layer $z = 1$. The chains grow only outside the core, that is, they are not allowed to enter the layer $z = 0$ (Scheme 1). All lattice sites unoccupied by the core or PMA units are occupied by solvent.

Because we use the lattice SCF calculations, the length of the lattice constant, l_{SCF}, must be judiciously set, and the number of effective lattice segments, n_{SCF}, has to be recalculated to allow a comparison with experimental data. Both parameters were estimated iteratively by comparing the experimental and cal-

SCHEME 1. Model of the Shell of Block Copolymer Micelle[a]

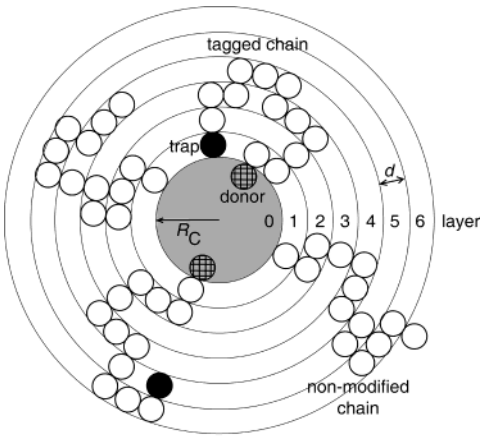

[a] The micellar core (shadowed) is modeled as an impenetrable sphere with a radius R_c. All chains in the shell are grafted to the core surface (their first segments are localized in layer 1) and are not allowed to enter into the core (layer 0). Tagged chains are terminated by pendant energy traps (black segments) and energy donors (square patterned segments) are localized in the core/shell interface; d is the lattice constant.

culated values of the radius of gyration of micellar shells formed by chains with several different contour lengths, L_{con}. After the first estimate of the lattice constant l_{SCF} had been done, an effective number of lattice segments was calculated from the contour length, $L_{con} = n_{PMA}l_{PMA} = n_{SCF}l_{SCF}$, where n_{PMA} is the real number of monomeric units of the PMA block and l_{PMA} is the contour length of the PMA unit. Then the radius of gyration of the shell, $R_{g,shell}^{SCF}$, was calculated by SCF using the interaction parameters described below and compared with experimental values calculated from the equation

$$R_{g,shell}^{exp} = \{^3/_5(R_h^5 - R_c^5)/(R_h^3 - R_c^3)\}^{1/2} \quad (9)$$

where hydrodynamic radii, R_h, were obtained from an empirical formula published by Qin and Munk and co-workers[53]

$$R_h = 0.347 n_{PS}^{0.71} n_{PMA}^{0.09} \quad (10)$$

The calculation was repeated for a set of copolymers differing in the length of the soluble block until experimental values of $R_{g,shell}^{exp}$ were not reproduced with the precision better than 5%. The final values of the optimized parameters for PS−PMA micelles formed by chains of PS block length 300 monomeric units and PMA block length 330 monomeric units are $d = 1.65$ nm, $n_{SCF} = 56$, $N_{ag} = 131$, and $R_c = 11.55$ nm.

The following values of the Flory−Huggins interaction parameters were used for reversible micelles in a mild 1,4-dioxane (80%)−water mixture: (i) The most important parameter, which controls the core size, $\chi_{CORE-SOLVENT}$, was set to 5.0. This value reflects the fact that the mixture is a bad solvent for PS. Its further increase has very little influence on the core dimensions and almost no influence on the shell structure, which was confirmed by a series of calculations. (ii) The parameter $\chi_{CORE-PMA}$ was found to have negligible effect on the shell structure and therefore was not considered to reduce the number of parameters, the influence of which has to be investigated. (iii) The parameter $\chi_{PMA-SOLVENT}$ plays an important role in the behavior of micellar systems. It controls the quality of the solvent for the shell. It was set to 0.0 for a relatively mild selective solvent 1,4-dioxane 80%−water.

Because the fluorometric experiments that we are interested in were performed in a mixture with 70% of water,[42−44] that is, in a solvent that differs from that used for the parametrization described above, we had to reparametrize our simulations. This approach was necessary because the above given empirical formulas for the size and molar mass of micelles have been published for a 1,4-dioxane mixture with 20% H_2O only, that is, for a mild selective solvent, where micelles coexist in reversible equilibrium with a low concentration of unimers and where an exchange of chains between micelles takes place. This means that the only solvent for which we are able to set reasonable values of l_{SCF} and n_{SCF} directly is the mixture with 20% H_2O. Nevertheless, the reparametrization may be achieved relatively easily for kinetically frozen micelles studied in our paper. Because the system is kinetically frozen, the association number does not change with increasing water content. Only the radius of gyration of the micellar shell changes. In this case, the value of the PMA−solvent interaction parameter, $\chi_{PMA-SOLVENT}$, controls the solvent quality for the shell. An increase in the water content, which is a very poor solvent for PS and a marginal solvent for PMA (in both nonelectrolyte and low-pH electrolyte regimes), deteriorates slightly the quality of the mixed solvent. The change in solvent quality may be described by increasing values of $\chi_{PMA-SOLVENT}$. A proper value of this interaction parameter, has to yield the radius of gyration identical with that calculated from experimental R_h for a mixture with 70% H_2O.[54] The value $\chi_{PMA-SOLVENT} = 1.1$ was obtained for a mixture with 70% H_2O.

In computer simulations of the shell structure and fluorescence data for hydrophobically modified systems (see below), the donor and acceptor (trap) characteristics have to be considered in the model. In real systems, the donors are located between PS and PMA blocks and represent the first segments of PMA chains (see Scheme 1). The acceptors are the last segments of PMA chains. Both, the donor and acceptor are strongly hydrophobic, and therefore, we assume that their interaction parameters with other components of the system are in most cases similar to those of the core. For the donor, which is incorporated in the core/shell interface, we assume exactly the same interaction parameters as those describing interactions of the core with other components. As concerns anthracene, its solubility in aqueous-rich media is appreciably lower than that of naphthalene, and therefore, we use a fairly high value $\chi_{TRAP-SOLVENT} = 10.0$. This value allows for reproducing high experimental values of the nonradiative steady-state energy transfer efficiency from donors and traps obtained for micelles formed by 100% tagged chains. To justify this strongly unfavorable value of the interaction parameter, we performed a series of parametric studies for a fairly broad region of this interaction parameter from 5.0 to 15.0, keeping other parameters constant. The obtained results, such as the size of micelles, are only little sensitive to this change, but as expected, an increase in $\chi_{TRAP-SOLVENT}$ slightly promotes the return of modified ends toward the core and increases the NRET effect. The interaction parameters of anthracene and PS core with other components (except the solvent) are identical. The values of all parameters presented in the system are recapitulated in Table 1.

Results and Discussion

Figure 1 shows the overall densities of segments of shell-forming PMA blocks in PS−PMA micelles as functions of the radial distance from the center of the spherical PS core. Individual curves show segment densities in shells of reference and hybrid micelles containing different fractions of tagged

TABLE 1: Optimized Values of Parameters Used for SCF Calculations of Hydrophobically Modified Micellar Shell[a]

micelle parameter	value	interaction parameter	value
lattice constant, d	1.65 nm	$\chi_{CORE-SOLVENT}$	5.0
core radius, R_c	11.55 nm	$\chi_{CORE-PMA}$[b]	0.0
agregation number, N_{ag}	131	$\chi_{TRAP-PMA}$	0.0
effective number of segments, n_{SCF}	56	$\chi_{CORE-TRAP}$[b]	0.0
		$\chi_{PMA-SOLVENT}$	1.1
		$\chi_{TRAP-SOLVENT}$	10.0

[a] Molecules of the solvent occupy all lattice sites that are not occupied by the core nor PMA units. [b] The parameters $\chi_{CORE-PMA}$ and $\chi_{CORE-TRAP}$ have a negligible effect on the shell structure and NRET and therefore were not optimized.

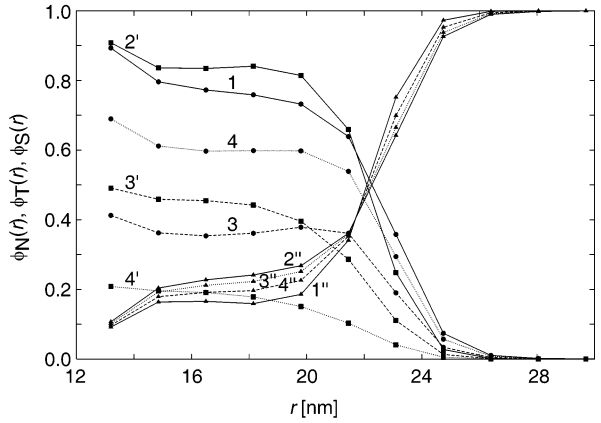

Figure 1. Density of segments of the shell-forming PMA blocks and solvent molecules as a function of the radial distance from the center of hybrid micelles containing different fractions of tagged PMA−A chains. Segments densities of nonmodified blocks, $\phi_N(r)$ (curves 1, 3, 4), of tagged blocks, $\phi_T(r)$ (2′, 3′, 4′), and of solvent molecules, $\phi_S(r)$ (1″, 2″, 3″, 4″) are shown. Curves 1 and 1″ correspond to nonmodified micelles, curves 2′ and 2″ correspond to 100% tagged micelles, curves 3, 3′, and 3″ correspond to micelles containing 50% tagged blocks, and curves 4, 4′, and 4″ correspond to micelles containing 20% tagged blocks.

PMA-A chains. Curve 1 corresponds to the nonmodified (reference) micellar system, $\phi_N(r)$ and curve 2′ to the 100% tagged micelles, $\phi_T(r)$. It is evident that the density in the inner and middle parts of the shell is higher for the tagged system. The shell density at the periphery is lower for the tagged system as compared with the nontagged reference system, but the ends of some chains stretch approximately to the same distance in both systems. Curves 3 and 3′ show segment densities of nontagged and tagged chains, $\phi_T(r)$ and $\phi_N(r)$, respectively, in a system composed of 50% of both types of chains, and curves 4 and 4′, respectively, depict the same dependences for a system composed of 20% tagged and 80% nontagged chains. A comparison of curves 3 and 3′ for the 1:1 system reveals immediately that the conformations of tagged chains are more collapsed and their segments cumulate in the inner and medium parts of the shell as compared with their nontagged counterparts. Curves 1″ to 4″ show solvent densities, $\phi_S(r)$, in individual systems. They are complementary to the total density of segments, that is, in hybrid systems they may be calculated as follows: $\phi_S(r) = 1 - (\phi_T(r) + \phi_N(r))$, where $\phi_T(r)$ and $\phi_N(r)$ are segment densities of tagged and nontagged chains, respectively.

In Figure 2, the densities of chain ends, $\phi_{TE}(r)$ and $\phi_{NE}(r)$, are shown as functions of the distance r from the core center for the same systems as in the previous figure. Curves 1 and 2′ depict the density of end segment in the reference PS−PMA system and the density of tags in the 100% tagged system, respectively. Curve 2′ for the 100% tagged system is shifted to significantly lower distances, and the density of tags very close to the core is appreciably higher than that for the free ends in the reference system. A comparison of individual curves shows that the hydrophobic tags tend to return toward the core and their fraction increases in the immediate vicinity of the core/shell interface in comparison with ends of nontagged chains. This fact explains high values of the energy transfer efficiency observed in our experimental works. The comparison of curves 3 and 3′, which show the density of tagged and nontagged chain ends, is very instructive. The numbers of both types of chains are the same in this system, and this allows for a fast and straightforward comparison. The curves show that the tagged and nontagged chains do behave quite differently.

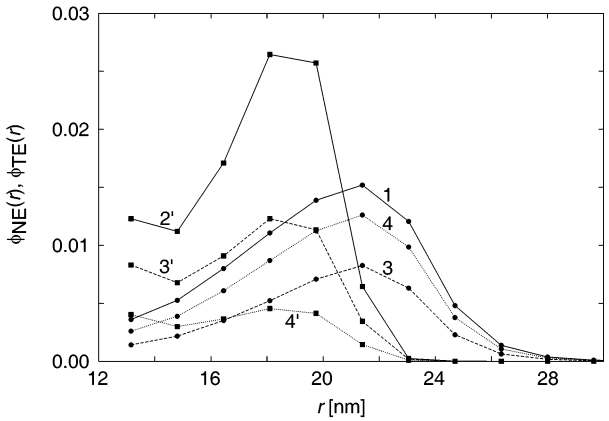

Figure 2. Density of chain ends as a function of the radial distance from the center of micelles for nonmodified blocks, $\phi_{NE}(r)$, and for tagged blocks, $\phi_{TE}(r)$. Numbering of curves is the same as in Figure 1.

The results presented in Figures 1 and 2 support our intuitive conclusion that we proposed on the basis of our experimental fluorometric studies. The hydrophobic traps try to bury in the inner shell close to the core because the polarity of this medium is lower than that of the solvent forcing the tagged chains to loop back and adopt relatively collapsed conformations. Because the formation of partially collapsed chain conformations is entropically unfavorable, the distribution of traps in the shell is a result of the enthalpy-to-entropy interplay. In fully tagged systems, the loops are relatively loose. In partly tagged systems, the nontagged chains are not affected and may adopt entropically favorable conformations. They compensate the entropy loss of the whole system and allow the tagged chains to collapse more. It is why higher fractions of tags may come close to the core/shell interface in partly tagged systems.

To demonstrate this behavior more clearly, we plotted the probability functions, $P_T(r)$ and $P_N(r)$, of finding a tagged chain end or a nontagged chain end in a distance r from the core center in Figure 3. The functions are normalized per one chain, which simplifies the comparison for systems with different degrees of tagging. The numbering of curves is the same as in previous figures. Besides the clear difference in the behavior of tagged and nontagged chains, we see that the probability of finding a tag in the vicinity of the core increases with decreasing degree of tagging.

Simulation of NRET. The results of our SCF calculations allow for simulations of NRET effect in hybrid double-tagged micellar systems with different degrees of tagging. However, one more parameter has to be considered, that is, the Förster radius, R^0, for the direct energy transfer from the donor (naphthalene) to the trap (anthracene).[55] From the point of view

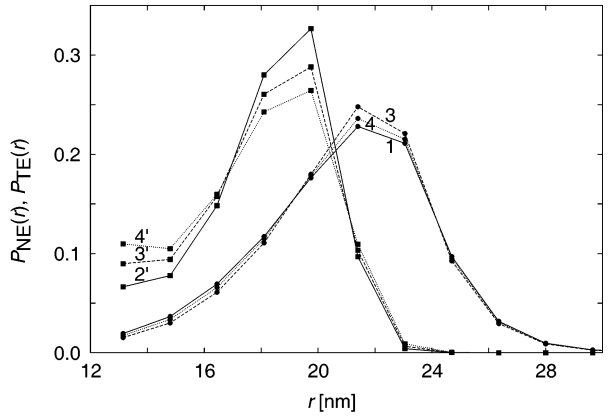

Figure 3. Probability density of finding the end of a nonmodified block, $P_{NE}(r)$, and the end of a tagged block (trap), $P_{TE}(r)$ in the distance r from the center of a micelle. Numbering of curves is the same as in Figure 1.

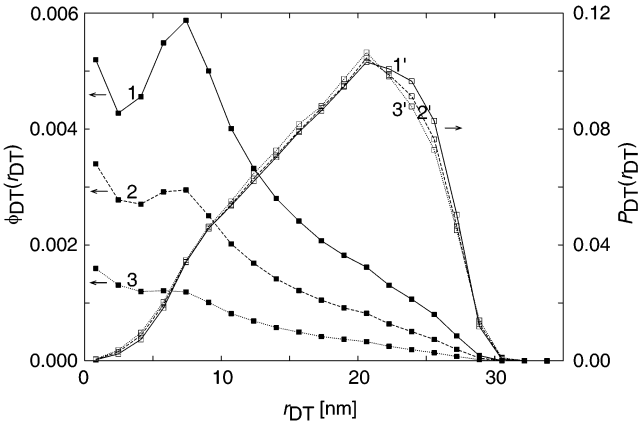

Figure 4. The probability of finding a tagged end in the distance r_{DT} from the excited donor, $P_{DT}(r_{DT})$, proportional to the number fraction of tagged ends (curves flagged by apostrophe) and the corresponding probability density (per unit volume), $\phi_{DT}(r_{DT})$. Curves 1 and 1′ describe the 100% tagged micelles, curves 2 and 2′ describe micelles containing 50% tagged blocks, and curves 3 and 3′ describe micelles containing 20% tagged blocks.

of the computer study (and the above-described parametrization), the Förster radius represents an extra thermodynamic parameter because it has no connection to the equilibrium size and behavior of micelles. Because there does not exist any theoretical background indicating whether this NRET characteristics should or should not be optimized (i.e., reparametrized) and how, we simply use the experimental value, $R^0 = 2.1$ nm.[56] We are aware of the fact that it may affect numerical results, because this value is only slightly higher than d and may limit the approach of traps to the donor and lower the calculated values of the energy transfer efficiency. Nevertheless, we believe that it should neither invalidate nor strongly affect general trends of the fluorescence behavior.

For the calculation of the excitation energy transfer from randomly excited donors to traps, we assume that, under current conditions applied in fluorometric measurements, maximum one donor per micelle is excited. Figure 4 shows the probability of finding the tagged end in the distance r_{DT} from an excited donor, $P_{DT}(r_{DT})$, together with the corresponding density normalized per unit volume, $\phi_{DT}(r_{DT})$, calculated as the number of traps in a layer with the center in the donor divided by the volume of this layer (see Scheme 2). The probability density, $\phi_{DT}(r_{DT})$, shows a double-peak shape. The maximum for small donor−trap separations is a result of a combined effect of favorable

SCHEME 2. The Evaluation of the Distribution Function of Donor−Trap Distances[a]

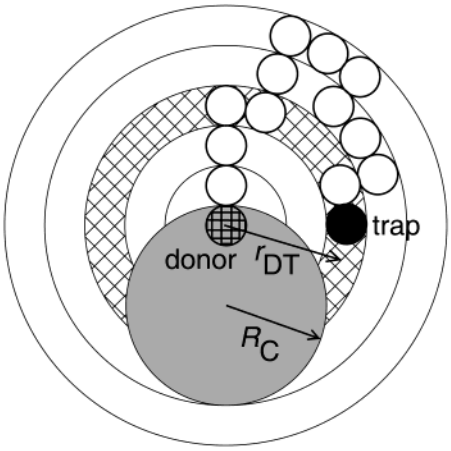

[a] The value of $N_{DT}(r_{DT})$ for a given r_{DT} is calculated as a number of traps in a spherical layer with a radius r_{DT} around the donor, divided by the volume of this layer, excluding the intersection with the core (inaccessible volume for traps).

core−trap interactions and unfavorable trap−solvent interactions. The second maximum at medium distances between 5 and 10 nm reflects the most important general trend of the behavior of the system and is due to unfavorable trap−solvent interactions alone. Because they are worse than interactions of the trap with all other components, the traps prefer contacts with PMA segments to those with the solvent and bury in a relatively dense part of the shell.

Using the distribution function of traps around a random excited donor, $P_{DT}(r_{DT})$, obtained by means of SCF calculations, the time-resolved donor emission, $I_D^q(t)$, and the energy transfer efficiency, χ^{tr}, may be calculated according to the well-known formulas[57]

$$I_D^q(t) = I_0 \exp\left\{-\frac{t}{\tau_D}\right\}\left[\int_0^{R_{ef}} \exp\left\{-\left[\frac{R_0}{r}\right]^6\left[\frac{t}{\tau_D}\right]\right\}P_{DT}(r_{DT})\,dr\right]^{N_T} \quad (11)$$

$$\chi^{tr} = \frac{R_0^6\int_0^{R_{ef}}\frac{P_{DT}(r_{DT})}{r_{DT}^6}\,dr}{R_0^6\int_0^{R_{ef}}\frac{P_{DT}(r_{DT})}{r_{DT}^6}\,dr + \frac{1}{N_T}} \quad (12)$$

where I_0 is the emission intensity immediately upon excitation at $t = 0$, τ_D is the fluorescence lifetime of the donor in the absence of traps, R^0 is the corresponding Förster radius, and R_{ef} is the radius of the effective sphere that contains N_T traps to which the transfer can occur.

Curves 1−3 in Figure 5 show the normalized fluorescence decays, $I_D^q(t/\tau_D)/I_0$, as functions of the reduced time, t/τ_D, calculated on the basis of eq 12, for systems with 100% (1), 50% (2), and 20% (3) tags. Curve 4 shows the fitted experimental fluorescence decay for the 100% tagged system together with the scatter in experimental data. In our earlier studies, we pointed out that the experimental decay for PS−N−PMA−A micelles has a peculiar shape as compared with the NRET-quenched decays for other polymeric, as well as low-molar-mass, systems.[43,44] It is strongly quenched at early times and only little affected at longer times. When we analyzed this decay curve, we compared it with theoretical decays simulated for

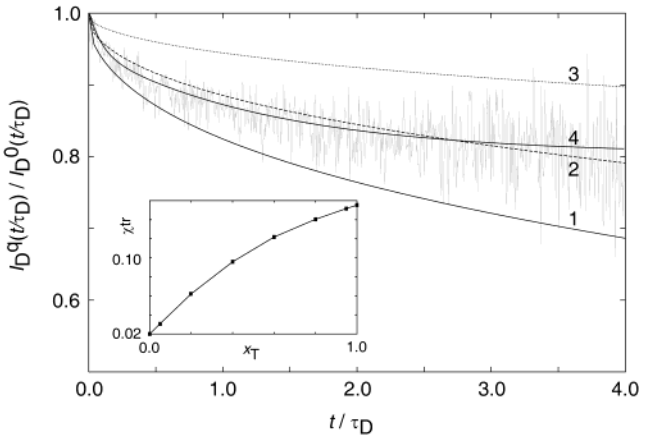

Figure 5. Time-resolved donor emission, $I_D^q(t)/I_D^0(t)$ for the 100% tagged micelle (curve 1), micelle containing 50% tagged blocks (2), and micelle containing 20% tagged blocks (3). The experimental decay for a system with 100% tagging is depicted by a dotted curve 4, together with experimental fluctuations. The inset shows the nonradiative energy transfer efficiency, χ^{tr}, as a function of the molar fraction of tagged chains, χ_T.

several physically reasonable distributions of traps in the shell (Gaussian, Maxwellian, etc.). These attempts failed to reproduce the experimental decay completely indicating that the distribution of traps is very different from those considered (tentatively, we suggested a possibility of a double-peak distribution). As shown above, the double-peak distribution was obtained by SCF calculations. Therefore, the SCF-simulated decay curves reproduce the experimental shape reasonably well at the semiquantitative level. It is evident that the calculated quenching effect is overestimated because the experimental curve compares better with the theoretical curve for the 50% tagged system and that the difference in slopes for early and long times is smaller as compared with the experimental curve. Nevertheless, the reproduction of the shape is reasonable and considerably better than that based on physically justifiable single-mode distribution functions.

Comparison of Theoretically and Experimentally Observed Trends. Results of SCF computer calculations confirm basic trends of the behavior of hydrophobically modified PS−PMA micellar systems that we reported in our earlier experimental studies.[30,42−44] The hydrophobic traps attached at the ends of PMA chains return back in the inner shell, forcing the tagged chains to loop toward the PS core or adopt partially collapsed conformations. The SCF calculations do not, in principle, allow for differentiation between these two types of conformations, but they show clearly a significant cumulating of segments of tagged PMA chains in the inner shell, close to the PS core.

The calculations performed so far do not reproduce the experimentally observed difference in sizes of fully tagged and nontagged systems. There are several potential reasons for this discrepancy. (i) The behavior of PMA in water-rich media is very complex and resembles that of polysoaps.[45−50] (ii) The experimental study was performed in a mixed solvent, and the preferential sorption of 1,4-dioxane in the inner shell may have produced a gradient in the solvent composition across the shell. The model simulations are simplified and neither capture all details of PMA behavior nor take the preferential sorption into account. However, on the basis of the majority of results, we believe that the computer study reproduces all decisive properties of micelles fairly well, and therefore, we do not think that the simplification of the model with respect to items i and ii is the main source of the above-mentioned differences. There are experimental reasons that may explain the observed difference. (iii) The experimentally studied samples, that is, the end-tagged PS−N−PMA−A and the nontagged PS−N−PMA were similar but not identical. Even though the length of the PMA blocks was almost the same in both copolymers, the PS block was longer in the former sample. The difference was not large, but it was not negligible. The estimates of the association numbers and sizes of micelles in an aqueous mixture with 80% 1,4-dioxane (scaling laws 8 and 10) show that both characteristics should be larger for micelles formed by the former copolymer than those for the latter sample, which agrees with what was observed experimentally. (iv) A slightly different polydispersity of micellar sizes confirmed by atomic force microscopy (AFM)[30] may result in a difference in sizes measured by light scattering techniques. Hence, we believe that the difference in sizes measured by QELS was caused mainly by a combination of complicating experimental factors iii and iv and that SCF calculations describe the sizes reasonably.

The computer study shows that the tagged PMA chains are more collapsed in hybrid (i.e., in only partially tagged) systems than those in a fully tagged system because the overall decrease in entropy is compensated by the behavior of nontagged chains. Hydrophobic traps (anthracene) come closer to the core/shell interface where the donors (naphthalene) are located, and this promotes the NRET effect. The simulated probabilities of finding a trap in the vicinity of the core normalized per chain (see Figure 3) are higher in hybrid systems in comparison with those in a 100% tagged system. However, the NRET increase is less pronounced than that observed in our experimental study. The NRET efficiency decreases with decreasing fraction of tagged chains. Presumably an easier collapse of tagged chains and the resulting increase in the number of more closely located donor−trap pairs is overbalanced by the decrease in the number of fluorophores.

In the experimentally studied micellar systems, we observed almost the same energy transfer efficiency in 20% and 100% tagged systems. This means that the collapse of tagged chains and a close approach of traps to the core play more important roles in the experimental system than the decrease in the number of fluorophores. The strong NRET in the experimental system may be caused by the polydispersity effect because we found by AFM that the polydispersity in sizes of hybrid micelles is significantly higher than that of single-component micelles.[30] Because the lengths of blocks in tagged and nontagged samples differ, we may expect that the polydispersity correlates with the heterogeneity in composition of micelles. In such a case, the resulting combined effect could become quite important.

From the purely theoretical point of view, the experimentally observed effect may be slightly suppressed in SCF calculations because of relatively short length of the reparametrized chains. We performed a series of simulations for different lengths of PMA chains. We found that the increasing length of chains causes larger differences in the conformational behavior of tagged and nontagged chains and promotes the NRET effect. This is a reasonable finding because the reduced length of chains together with their limited flexibility at the simple cubic lattice is expected to suppress the entropy-driven effects.

In any case, the basic qualitative trends and the main features of the conformational behavior of both types of chains in hybrid systems were reproduced correctly in the SCF study. The comparison shows that the SCF model reproduces all decisive trends and main features of the conformational behavior of both types of chains in the reference nonmodified micellar systems, in 100% modified and in partly modified systems, well at the

qualitative and in most cases also at the semiquantitative level. As concerns the quantitative comparison, there is still room for improvement. Computer studies, both SCF and MC simulations, are in progress and results will be published soon because it is interesting to compare details of the behavior found by two independent methods.

Conclusions

(1) We performed a parametrized SCF study of hydrophobically modified polymeric PS−PMA micelles in 1,4-dioxane−water mixtures. The parametrization is based on the reproduction of structural characteristics of nonmodified micelles. (2) The study shows that the end-attached hydrophobic tags (anthracene) try to escape the polar solvent and bury in the inner PMA shell, forcing the PMA chains to loop back toward to PS core. (3) In partly modified systems, the tagged and nontagged chains show different conformational behavior. Because the entropy decrease due to formation of chain loops and collapsed conformations is compensated by the behavior of nontagged chains, a higher fraction of tags return closer to the PS cores as compared with the 100% tagged systems. (4) The SCF study allows for the calculation of NRET and fluorescence decay curves in double-tagged systems containing energy donors in the core/shell interface and pendant traps at the ends of PMA chains. Theoretical decay curves, based on the donor-trap distributions obtained by SCF, reproduce the experimental fluorescence decays reasonably well at the semiquantitative level.

Acknowledgment. The study is a part of the long-term Research Plan of the School of Science of the Charles University in Prague No. MSM 113100001. Authors thank the Laboratory of Physical Chemistry and Colloid Science at Wageningen University, The Netherlands, namely, Dr. F. A. M. Leermarkers and Prof. G. J. Fleer, for providing their software for SCF calculations. This study was supported by the Ministry of Education of the Czech Republic (Grant No. FRVS/2265/2002), by the Grant Agency of the Czech Republic (Grant No. 203/01/0536 and No. 203/03/0262), and by the Grant Agency of the Charles University (Grant No. 215/2000/BCh/PrF). The numerical calculations were performed by using the computer facilities of the Computer Meta-Center (Praha-Brno-Plzeň) of the Ministry of Education of the Czech Republic.

References and Notes

(1) Tuzar, Z.; Kratochvíl, P. In *Surface and colloid science*; Matievic, E., Ed.; Plenum Press: New York, 1993; Vol. 15, p 1.
(2) Khougaz, K.; Astafieva, I.; Eisenberg, A. *Macromolecules* **1995**, *28*, 7135.
(3) Zhang, L. F.; Eisenberg, A. *Macromolecules* **1999**, *32*, 2239.
(4) Shen, H. W.; Eisenberg, A. *J. Phys. Chem. B* **1999**, *103*, 9473.
(5) Antonietti, M.; Förster, S.; Oestreich, S. *Macromol. Symp.* **1997**, *121*, 75.
(6) Wooley, K. L. *J. Polym. Sci., Part A: Polym. Chem.* **2000**, *38*, 1397.
(7) Butun, V.; Lowe, A. B.; Billingham, N. C.; Armes, S. P. *J. Am. Chem. Soc.* **1999**, *121*, 4288.
(8) Narrainen, A. P.; Pascual, S.; Haddleton, D. M. *J. Polym. Sci., Part A: Polym. Chem.* **2002**, *40*, 439.
(9) Cheng, G. L.; Boker, A. A.; Zhang, M. F.; Krausch, G.; Müller, A. H. E. *Macromolecules* **2001**, *34*, 6883.
(10) Kataoka, K.; Harashima, H. *Adv. Drug Delivery Rev.* **2001**, *52*, 151.
(11) Yamamoto, Y.; Nagasaki, Y.; Kato, Y.; Sugiyama, Y.; Kataoka, K. *J. Controlled Release* **2001**, *77*, 27.
(12) Nagasaki, Y.; Yasugi, K.; Yamamoto, Y.; Harada, A.; Kataoka, K. *Biomacromolecules* **2001**, *2*, 1067.
(13) Hennink, W. E.; van Nostrum, C. F. *Adv. Drug Delivery Rev.* **2002**, *54*, 13.
(14) Neradovic, D.; van Nostrum, C. F.; Hennink, W. E. *Macromolecules* **2001**, *34*, 7589.
(15) de Jong, S. J.; De Smedt, S. C.; Demeester, J.; van Nostrum, C. F.; Kettenes-van den Bosch, J. J.; Hennink, W. E. *J. Controlled Release* **2001**, *72*, 47.
(16) Neradovic, D.; Hinrichs, W. L. J.; Kettenes-van den Bosch, J. J.; van Nostrum, C. F.; Hennink, W. E. *J. Controlled Release* **2001**, *72*, 252.
(17) de Jong, S. J.; van Eerdenbrugh, B.; van Nostrum, C. F.; Kettenes-van de Bosch, J. J.; Hennink, W. E. *J. Controlled Release* **2001**, *71*, 261.
(18) Nishiyama, N.; Kataoka, K. *J. Controlled Release* **2001**, *74*, 83.
(19) Nishiyama, N.; Yokoyama, M.; Aoyagi, T.; Okano, T.; Sakurai, Y.; Kataoka, K. *Langmuir* **1999**, *15*, 377.
(20) Katayose, S.; Kataoka, K. *Bioconjugate Chem.* **1997**, *8*, 702.
(21) Munk, P.; Procházka, K.; Tuzar, Z.; Webber, S. E. *CHEMTECH* **1998**, *28*, 20.
(22) Kiserow, D.; Procházka, K.; Ramireddy, C.; Tuzar, Z.; Munk, P.; Webber, S. E. *Macromolecules* **1992**, *25*, 461.
(23) Procházka, K.; Kiserow, D.; Ramireddy, C.; Tuzar, Z.; Munk, P.; Webber, S. E. *Macromolecules* **1992**, *25*, 454.
(24) Ramireddy, C.; Tuzar, Z.; Procházka, K.; Webber, S. E.; Munk, P. *Macromolecules* **1992**, *25*, 2541.
(25) Tsitsilianis, C.; Voulgaris, D.; Štěpánek, M.; Podhájecká, K.; Procházka, K.; Tuzar, Z.; Brown, W. *Langmuir* **2000**, *16*, 6868.
(26) Štěpánek, M.; Procházka, K.; Brown, W. *Langmuir* **2000**, *16*, 2502.
(27) Lee, A. S.; Gast, A. P.; Butun, V.; Armes, S. P. *Macromolecules* **1999**, *32*, 4302.
(28) Shen, H. W.; Zhang, L. F.; Eisenberg, A. *J. Am. Chem. Soc.* **1999**, *121*, 2728.
(29) Shen, H. W.; Eisenberg, A. *Macromolecules* **2000**, *33*, 2561.
(30) Matějíček, P.; Humpolíčková, J.; Procházka, K.; Tuzar, Z.; Špírková, M.; Hof, M.; Webber, S. E. *J. Phys. Chem. B* **2003**, *107*, 8232.
(31) Procházka, K. *J. Phys. Chem.* **1995**, *99*, 14108.
(32) Viduna, D.; Limpouchová, Z.; Procházka, K. *Macromolecules* **1997**, *30*, 7263.
(33) Limpouchová, Z.; Viduna, D.; Procházka, K. *Macromolecules* **1997**, *30*, 8027.
(34) Jelínek, K.; Limpouchová, Z.; Procházka, K. *Macromol. Theory Simul.* **2000**, *9*, 703.
(35) Shusharina, N. P.; Nyrkova, I. A.; Khokhlov, A. R. *Macromolecules* **1996**, *29*, 3167.
(36) Khalatur, P. G.; Khokhlov, A. R.; Nyrkova, I. A.; Semenov, A. N. *Macromol. Theory Simul.* **1996**, *5*, 713.
(37) Wijmans, C. M.; Zhulina, E. B. *Macromolecules* **1993**, *26*, 7214.
(38) Linse, P. *J. Phys. Chem.* **1993**, *97*, 13896.
(39) Wijmans, C. M.; Linse, P. *Langmuir* **1995**, *11*, 3748.
(40) Svensson, M.; Alexandridis, P.; Linse, P. *Macromolecules* **1999**, *32*, 637.
(41) Viduna, D.; Milchev, A.; Binder, K. *Macromol. Theory Simul.* **1998**, *7*, 649.
(42) Matějíček, P.; Uhlík, F.; Limpouchová, Z.; Procházka, K.; Tuzar, Z.; Webber, S. E. *Collect. Czech. Chem. Commun.* **2002**, *67*, 531.
(43) Uhlík, F.; Limpouchová, Z.; Matějíček, P.; Procházka, K.; Tuzar, Z.; Webber, S. E. *Macromolecules* **2002**, *35*, 9497.
(44) Matějíček, P.; Uhlík, F.; Limpouchová, Z.; Procházka, K.; Tuzar, Z.; Webber, S. E. *Macromolecules* **2002**, *35*, 9487.
(45) Katchalski, A. *J. Polym. Sci.* **1951**, *7*, 393.
(46) Anufrieva, E. V.; Birshtein, T. M.; Nekrasova, T. N.; Ptitsyn, C. B.; Scheveleva, T. V. *J. Polym. Sci., Part C* **1968**, *16*, 3519.
(47) Ghighino, K. P.; Tan, K. L. In *Polymer Photophysics*; Philips, D., Ed.; Chapman and Hall: London, 1985; Chapter 7.
(48) Wang, Y. C.; Morawetz, H. *Macromolecules* **1986**, *19*, 1925.
(49) Bednář, B.; Trněná, J.; Svoboda, P.; Vajda, Š.; Fidler, V.; Procházka, K. *Macromolecules* **1991**, *24*, 2054.
(50) Soutar, I.; Swanson, L. *Macromolecules* **1994**, *27*, 4304.
(51) Fleer, G. J.; Scheutjens, J. M. H. M.; Cohen Stuart, T. C. M. A.; Vincent, B. *Polymers at interfaces*; Chapman and Hall: London, 1993.
(52) van den Oever, J. M. P.; Leermakers, F. A. M.; Fleer, G. J.; Ivanov, V. A.; Shusharina, N. P.; Khokhlov, A. R.; Khalatur, P. G. *Phys. Rev. E* **2002**, *65*.
(53) Qin, A. W.; Tian, M. M.; Ramireddy, C.; Webber, S. E.; Munk, P.; Tuzar, Z. *Macromolecules* **1994**, *27*, 120.
(54) Munk, P.; Ramireddy, C.; Tian, M.; Webber, S. E.; Procházka, K.; Tuzar, Z. *Makromol. Chem., Macromol. Symp.* **1992**, *58*, 195.
(55) Förster, T. *Z. Naturforsh.* **1949**, *4a*, 321.
(56) Berleman, I. B. *Energy transfer parameters of aromatic compounds*; Academic press: New York, London, 1973.
(57) Mendelsohn, A. S.; Delacruz, M. O.; Torkelson, J. M. *Macromolecules* **1993**, *26*, 6789.